PHYSICAL REVIEW B **67**, 161306(R) (2003)

Pseudopotential calculation of the excitonic fine structure of million-atom self-assembled $In_{1-x}Ga_xAs/GaAs$ quantum dots

Gabriel Bester,[1] Selvakumar Nair,[2] and Alex Zunger[1]
[1]*National Renewable Energy Laboratory, Golden, Colorado 80401*
[2]*ECAN, University of Toronto, Toronto, Canada M5S3E3*
(Received 16 January 2003; published 30 April 2003)

The atomistic pseudopotential method is used to accurately predict the electron-hole exchange-induced fine structure (FS) and polarization anisotropy in million-atom $In_{1-x}Ga_xAs/GaAs$ quantum dots of various shapes and compositions. The origin of the FS splittings is clarified using a simple model where the effects of atomistic symmetry and spin-orbit interaction are separately evident. Remarkably, polarization anisotropy and FS splittings are shown to occur, even in a cylindrically symmetric dot. Furthermore, ''dark excitons'' are predicted to be partially allowed. Trends in splittings among different shapes and compositions are revealed.

DOI: 10.1103/PhysRevB.67.161306 PACS number(s): 73.21.La, 71.15.−m, 73.22.−f, 78.67.Hc

Recent advances in single-dot spectroscopy[1–6] revealed that the excitonic lines of self-assembled $In_{1-x}Ga_xAs/GaAs$ quantum dots exhibit a surprising fine-structure (FS) with unique polarization anisotropy.[4,7–9] Indeed the study of FS has become very important recently.[1,4,9] It was found that the spectra of (001)-grown lens-shaped dots break into a few sharp lines, ~0.1 meV apart, exhibiting pronounced *in-plane* anisotropy, distinguishing the seemingly equivalent [110] direction from the $[\bar{1}10]$. This is surprising in two ways. First, in spherical *colloidal* dots, the dipoles-allowed (''bright'') states do not exhibit FS.[10] Second, the measured spatial anisotropy[4–6,9] suggests a lower symmetry than the nominal shape symmetry of the dot, which is often a rotationally symmetric lens; whereas such low (e.g., C_{2v}) symmetries were predicted theoretically[11] and their effect on *single*-particle physics (e.g., P_x-P_y splitting) was discussed, the consequences of such symmetry on the many-body FS was not appreciated. Indeed, since continuum-type theories,[4,5,8,6] based on the classic envelope-function methodology,[12] completely lack FS for symmetric dots, the observation of FS[1,4] led to the suggestion that the dot must be geometrically asymmetric. We show here that even if the dot is geometrically symmetric (e.g., circular-based lens shaped), there is a FS and polarization anisotropy. Calculating this effect in self-assembled dots is a challenge: Unlike colloidal dots that include $\sim 10^3$ atoms, predicting the electronic and FS properties of self-assembled dots, including $\sim 10^6$ atoms (dot +barrier) is considerably more complex. Using an atomistic pseudopotential approach to the single-particle and many-body description of excitons in lens-shaped $In_{1-x}Ga_xAs/GaAs$ self-assembled quantum dots, we show here how the atomistic lattice symmetry combined with the electron-hole exchange interaction produces excitonic FS with pronounced in-plane polarization anisotropy even in cylindrically symmetric dots. Unlike continuum models which introduce a phenomenological *ad hoc* ''in-plane asymmetry parameter'' to fit to the measured splitting, we are able to provide quantitative *predictions* of the FS. Our theory naturally includes long- and short-range exchange interactions.

Monoexcitons in self-assembled quantum dots exhibit spectroscopic features on two energy scales: First, one observes the usual *exciton structure* with splittings on the 10–100 meV scale corresponding to the orbitally distinct (e.g., S_e-S_h vs P_e-P_h) Coulomb-stabilized electron(e)-hole(h) pairs. Second, one observes a *fine structure*, on a 0.01–1 meV scale, comprising of exchange-stabilized states *within* a given orbitally-distinct (e.g., S_e-S_h) exciton. Excitons in both energetic hierarchies can be described by combining the single-particle description with a many-body expansion. The underlying physics can be described and computed as follows.

The single-particle problem. The single-particle (orbital) levels of a quantum dot are obtained by solving the one-electron Schrödinger equation in a confining potential $V(\mathbf{r})$. Thus, we describe $V(\mathbf{r})$ as a superposition of strained atomic (pseudo) potentials centered at the atomic equilibrium[13,14] positions (for $\sim 2\times 10^6$ atoms). The eigenstates of $V(\mathbf{r})$ [obtained numerically within a basis of ''linear combination of Bloch bands (LCBB)''[15] including multiband and intervalley couplings] must transform like the irreducible representation of the point-group symmetry underlying the nanostructure. For lens-shaped or pyramidal-shaped dots, this atomistic symmetry is C_{2v} distinguishing the [110] from the $[\bar{1}10]$ direction, even if the overall shape is ''ideal,'' e.g., *circular*-base lens or *square*-base pyramid.[11] As a consequence of the atomistic symmetry, the electron and hole levels can be of mixed orbital and mixed Bloch character. These features are illustrated in Fig. 1 which analyzes the single-particle orbitals for a flat and a tall $In_{0.6}Ga_{0.4}As/GaAs$ dot in terms of the orbital character (S,P,D) and the Bloch character $[J_z = 3/2;\ 1/2;\ 1/2'$ and el, see caption of Fig. 1] of the wave functions. We see that the wave functions of the flat dot are close to what ideal continuum models would suggest: The ground hole state is 90% *S*-like, heavy-hole ($J_z = 3/2$) like, whereas the next two hole levels are ≈80% *P*-like and heavy-hole-like, with only 6–7% *S* or *D* character. The electron states have only weak interband coupling (around 6%) and almost pure orbital character. However, for the tall dot, the situation is similar for the electron states but dramatically different for the holes: even the ground-state hole has strongly mixed *S* (41%) and *P* (28%) character and is only 73% heavy-hole ($J_z = 3/2$) like. This enhanced mixing with

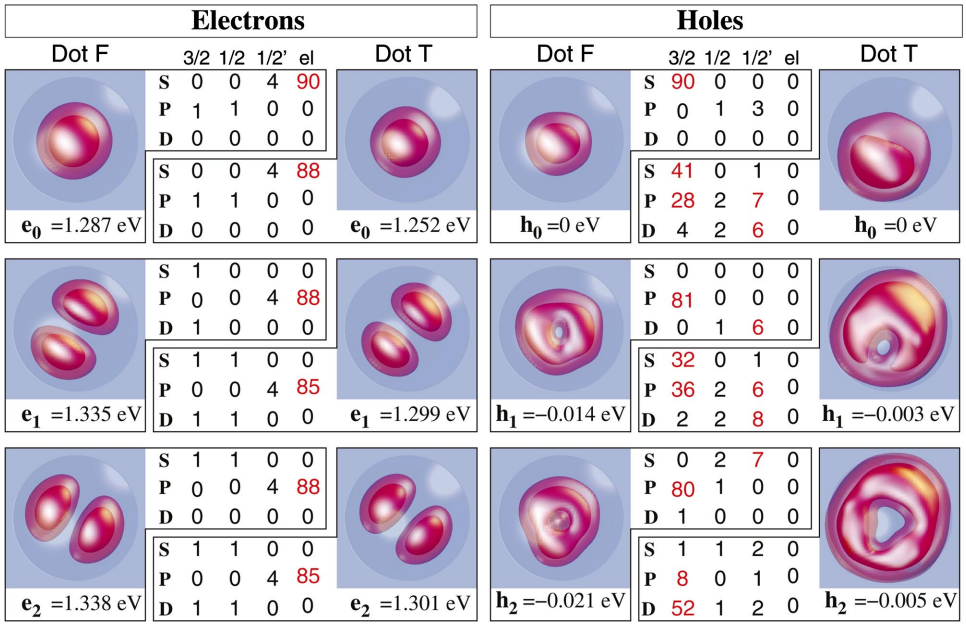

FIG. 1. (Color) Isosurfaces of the squared wave functions of the first three electron and first three hole states for a flat (dot *F*, 25.2 nm base and 3.5 nm height) and a tall (dot *T*, $b=25.2$ nm, $h=5$ nm) $In_{0.6}Ga_{0.4}As/GaAs$ dot. The two isosurfaces enclose 75% and 40% of the state densities. For analysis purposes, we project the wave functions on three valence bands *x*, *y*, *z*, and the lowest electron band el. The valence bands are labeled by their axial angular momentum values, $J_z=3/2$ for heavy hole, $J_z=1/2$ for $(x-iy)/\sqrt{2}\uparrow$, $(x+iy)/\sqrt{2}\downarrow$, and $J_z=1/2'$ for $z\uparrow$, $z\downarrow$. The wave functions are further decomposed with respect to their axial angular momentum components (*S*, *P*, *D*). Random alloy fluctuations have a strong effect on the visual shape of the hole states. However, the energies and the character of the wave functions remain nearly constant for different random alloys.

increasing height results from the fact that for tall dots the confinements in *x*-*y* and *z* directions are comparable revealing the true zero-dimensional properties. Interestingly, Fig. 1 shows that the magnitude of this mixing effect increases dramatically with only modest increase in height (from 3.5 nm to 5 nm).

Coulomb-stabilized excitonic structure. Each pair $|e_ih_j\rangle$ composed of a single-particle electron $(e_0,e_1,e_2,\ldots)$ and hole state $(h_0,h_1,h_2,\ldots)$ defines a single configuration. Including spin, this state is fourfold degenerate. The electron-hole Coulomb interaction $J(e_i,h_j)$ leaves this fourfold degeneracy intact, but binds the electron-hole pair. Correlations are introduced by allowing different single configurations $|e_ih_j\rangle$ to interact via configuration interaction (CI).[10] These correlations modify the FS splittings. The ensuing many-body states $\Psi_\alpha=\Sigma_{i,j}C_{ij}^{(\alpha)}|e_ih_j\rangle$ often contain a dominant configuration, i.e., one with a particularly large $|C_{ij}|^2$, which will be used to label excitonic states. The Coulomb and exchange matrix elements needed for the CI calculation are computed numerically[10] from 12 electron and 12 hole pseudopotential single-particle orbitals, and are screened by the dielectric function according to the model described in Ref. 16. Absorption is calculated by Fermi's golden rule applied to CI states. The calculated low-resolution spectra for a flat InAs/GaAs dot (Fig. 2, upper panel) show a single S_e-$S_h(e_0$-$h_0)$ line, followed by a maximum of four lines for the P_e-P_h channel, then the D_e-D_h channel. The width of the P_e-P_h channel is typically around 10 meV for cylindrical dots, but broadens to 27 meV for an elongated dot (dot *E* in Table I).

Exchange-induced FS. The *e*-*h Coulomb* interactions give rise to excitonic structure that can be labeled by different dominant orbital configurations $|e_ih_j\rangle$ of the CI states (e.g., upper part of Fig. 2), the *e*-*h exchange* interaction splits those states in a way that sensitively reflects the atomistic symmetry (lower part of Fig. 2). We calculated the FS splitting of four dots, and present the results in Fig. 2 and Table I. We see, in Fig. 2, that each peak in the excitonic spectra is split into four FS lines. Those shown in Fig. 2 as light (heavy) lines are ''dark'' (bright) excitons. *Remarkably, even the symmetric dots (denoted P, F, and T), show splitting of bright states as well as strong polarization anisotropy.*

To interpret the results, we develop a simple model for the case where the envelope-function part of the electron and

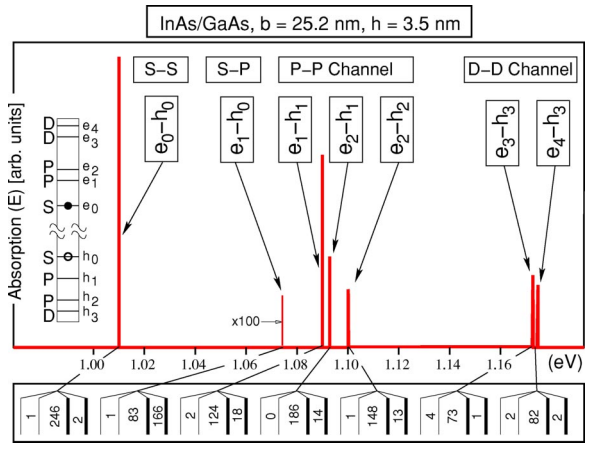

FIG. 2. Absorption spectra for a pure InAs dot (dot *P*). Upper panel: low-resolution excitonic structure. Weak transitions, apart from e_1-h_0, have been omitted. Lower panel: FS splittings in μeV. Thin (heavy) lines denote dark (bright) states.

TABLE I. FS splittings for three $In_{0.6}Ga_{0.4}As/GaAs$ dots: dot F ($b=25.2$ nm, $h=3.5$ nm), dot E (elliptical base with $b1=26$ nm, $b2=20$ nm, and $h=3.5$ nm), and dot T ($b=25.2$ nm, $h=5$ nm). The transition energies are in eV, while the FS splittings K, δ, η [see Fig. 3(d)] are in μeV. The dominant single-particle state contribution and the dominant orbital character of the excitons is denoted as e_i-h_i and L_e-L_h, respectively. The polarization P is given in percent for the low/high bright state.

Energy	e_i-h_j	L_e-L_h	K	2δ	2η	P
			Dot F			
1.266	0-0	S-S	164	4	0	−53/51
1.305	0-4	S-S	68	32	0	21/−20
1.334	1-1	P-P	85	9	1	13/−26
1.336	2-1	P-P	68	13	0	−65/68
1.341	1-2	P-P	109	26	3	−33/3
1.343	2-2	P-P	46	34	1	−97/92
1.399	3-3	D-D	44	6	1	−77/68
1.402	4-3	D-D	39	6	0	−91/90
			Dot E			
1.275	0-0	S-S	230	30	1	98/−98
1.340	1-1	P-P	125	12	0	−64/61
1.348	1-2	P-P	98	34	3	93/−95
1.360	2-1	P-P	95	11	1	−87/94
1.367	2-2	P-P	106	23	3	−70/83
1.410	3-3	D-D	61	3	0	−87/81
1.420	3-4	D-D	65	26	4	100/−100
1.427	4-3	D-D	42	9	0	−94/97
			Dot T			
1.237	0-0	S-S	122	9	0	100/−100
1.241	0-1	S-P	80	7	0	96/−96
1.285	1-0	P-S	66	77	1	−90/86
1.288	1-1	P-P	73	8	1	94/−95
1.291	2-1	P-P	64	33	1	−77/83

hole states are of Γ_1 (S-like) symmetry. The Bloch part of the electron state is of Γ_1 symmetry in zinc-blende structure. The electron states in the following are therefore, including spin, twofold (Kramer's) degenerate. Furthermore, the contribution of the valence $|Z\rangle$ band in the hole states is neglected since it is pushed down in energy through the strong confinement in z direction (for flat dots). We will proceed in steps from the idealized cylindrical symmetry neglecting at first the spin-orbit interaction [Fig. 3(a)], to the full atomistic symmetry (C_{2v}) in the presence of the spin-orbit interaction [Fig. 3(d)]. We will show how the observed FS is the result of the atomistic symmetry in presence of the spin-orbit interaction.

Cylindrical symmetry, no spin-orbit interaction [Figs. 3(a) and 4(a)]. In this case, the hole states are eigenfunctions of the angular momentum $l=1$ as depicted in Fig. 4(a). The spin parts of the wave functions are written as $|\uparrow\rangle$ and $|\downarrow\rangle$. Due to the equivalence of the wave functions $|X\rangle$ and $|Y\rangle$ in cylindrical symmetry, the four hole states are degenerate. The resulting eight exciton states (two electrons, four holes) are split by the exchange interaction K (singlet-triplet splitting) into two $S=0$ and six $S=1$ states.

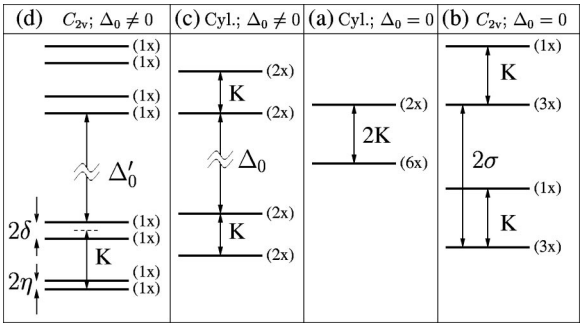

FIG. 3. Schematic evolution of the *excitonic* FS. Δ_0' and Δ_0 are the spin-orbit splitting energies in the presence and absence of the C_{2v} potential, σ is the atomistic asymmetry factor, and K is the exchange splitting energy (see text).

C_{2v} symmetry, no spin-orbit interaction [Figs. 3(b) and 4(b)]. The spin-independent C_{2v} potential does not have the ability to mix spins. However, it will mix the orbital parts of isospin hole states creating the eigenstates given in Fig. 4b, where the C_{2v} point-group notation[17] has been used. We obtain two pairs of eigenfunctions whose orbital parts belong to the Γ_2 and Γ_4 representations and spin parts to the Γ_5 representation. The splitting of these two pairs is due to the nonequivalence of the $|\Gamma_{2v}\rangle$ and $|\Gamma_{4v}\rangle$ Bloch functions (atomistic asymmetry), reflected in the atomistic asymmetry parameter $\sigma=\langle\Gamma_{2v}|H_{C_{2v}}|\Gamma_{2v}\rangle-\langle\Gamma_{4v}|H_{C_{2v}}|\Gamma_{4v}\rangle$, which is characteristic of the C_{2v} potential. The previously fourfold degenerate hole states split into two by 2σ. Consequently, the *exciton* states are split by the atomistic asymmetry 2σ and further split into singlet and triplet by the exchange term K [Fig. 3(b)].

Cylindrical symmetry, with spin-orbit interaction [Figs. 3(c) and 4(c)]. The spin-orbit interaction splits the hole states with respect to their total angular momentum J. Thus, the $J_z=3/2$ hole states $a\uparrow$ and $b\downarrow$ will split by Δ_0 from the $J_z=1/2$ states $a\downarrow$ and $b\uparrow$ [see Fig. 4(c)]. Considering only the first two hole states ($a\uparrow$, $b\downarrow$) and the electron states ($e\downarrow$, $e\uparrow$), the exchange Hamiltonian in the basis of the four excitons ($a\uparrow e\uparrow$), ($a\uparrow e\downarrow$), ($b\downarrow e\uparrow$) and ($b\downarrow e\downarrow$) is given by H_{ex} (H_{ex}' will be described later):

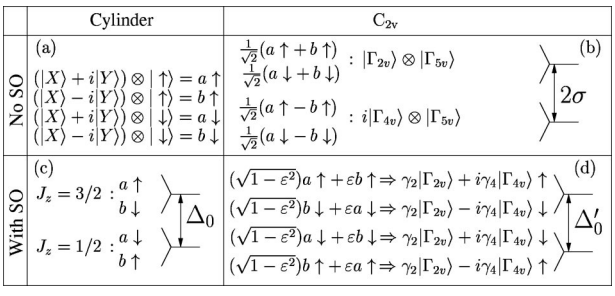

FIG. 4. Symmetry analysis of the single-particle *hole* state. Δ_0 is the spin-orbit splitting energy and σ is the atomistic asymmetry splitting energy (see text). With, $\gamma_2=(\sqrt{1-\varepsilon^2}+\varepsilon)/\sqrt{2}$, $\gamma_4=(\sqrt{1-\varepsilon^2}-\varepsilon)/\sqrt{2}$, and $\Delta_0'=\sqrt{\Delta_0^2+4\sigma^2}$.

$$H_{\mathrm{ex}}=\begin{pmatrix} 0 & 0 & 0 & 0 \\ 0 & \mathrm{K} & \delta & 0 \\ 0 & \delta & \mathrm{K} & 0 \\ 0 & 0 & 0 & 0 \end{pmatrix}, \quad H'_{\mathrm{ex}}=\begin{pmatrix} \eta & 0 & 0 & \eta \\ 0 & \mathrm{K} & \delta & 0 \\ 0 & \delta & \mathrm{K} & 0 \\ \eta & 0 & 0 & \eta \end{pmatrix} \quad (1)$$

since the e-h exchange interaction only affects $S=0$ states. In cylindrical symmetry $|X\rangle$ and $|Y\rangle$ are equivalent and the "bright exciton splitting" δ vanishes. The first four exciton states form two doublets separated by the exchange interaction K [Fig. 3(c)].

C_{2v} Symmetry, with spin-orbit interaction [Figs. 3(d) and 4(d)]: The C_{2v} potential, will allow mixing of isospin states [Fig. 4(d)]. However, this mixing, denoted by ε, will be weak since the isospin states are far in energy, shifted by the large spin-orbit interaction energy Δ_0. The eigenvectors of the new hole states are given in Fig. 4(d) using the a and b as well as in C_{2v} notation. Using the latter basis, the exchange Hamiltonian is still given by H_{ex} but with $\delta=\delta^0+2\varepsilon K^0\sqrt{1-\varepsilon^2}$ and $\mathrm{K}=K^0+2\varepsilon\delta^0\sqrt{1-\varepsilon^2}$. K^0 is half of the sum of $\langle\Gamma_{2v}\Gamma_{1e}|H_{\mathrm{ex}}|\Gamma_{2v}\Gamma_{1e}\rangle$ and $\langle\Gamma_{4v}\Gamma_{1e}|H_{\mathrm{ex}}|\Gamma_{4v}\Gamma_{1e}\rangle$, while δ^0 is half of the difference of both expressions and is, like σ, a measure of the atomistic asymmetry of the dot. The asymmetry σ leads to the mixing ε of the split-off states. ε is therefore proportional to σ and inversely proportional to Δ_0.

Our simple theoretical model identifies the microscopic meaning of the various splitting parameters K, σ, η and δ (Fig. 3). We now use this understanding to analyze the pseudopotential-CI calculated FS (lower panel of Fig. 2 and in Table I).

The splitting δ of the bright states. We observe larger splittings for transitions of the P_e-P_h and D_e-D_h channels ($9-46\ \mu$eV) than exhibited in the S_e-S_h channel ($2-30\ \mu$eV). The weak, "forbidden" e_S-h_P transition exhibits a surprisingly large ($166\ \mu$eV) splitting. Asymmetries in the overall dot shape tend to increase the splittings, as seen in Table I for dot E (elongated). Notably, even cylindrically symmetric dots (P,F,T) have nonzero splittings. Comparison with experiment is complicated by the fact that currently there are very few experimental characterizations of the size (especially the height), shape, and composition of the dots for which FS is reported. In Refs. 4 and 6, δ is between $0-150\ \mu$eV for the ground-state exciton. A value as large as $150\ \mu$eV is not predicted for the present dots (P,F,T,E), but is nevertheless conceivable for strongly elongated tall dots.

The polarization ratio $P=(I_{110}-I_{\bar{1}10})/(I_{110}+I_{\bar{1}10})$. The bright states are split and show strong polarization in [110] and [1$\bar{1}$0] directions. Even for circular-based lens-shaped dots we predict 100% polarization and show that measurements of finite polarizations can not be used as evidence for dot shape anisotropies. Notably, strong deviations from the expected 100% are found for certain transitions.

The singlet-triplet splitting K. The predicted values for K are in very good agreement with experiment. Bayer *et al.*[6] measure for the ground-states exciton $\mathrm{K}=116\ \mu$eV for a dot of $\approx$25 nm diameter and unspecified height. This value fits very well with the calculated 122 μeV for dot $T(b=25.2\ \mathrm{nm}, h=5\ \mathrm{nm})$. Furthermore we report larger values for K in strongly confined systems like in the elongated dot E (20 nm confinement in the x-y plane) and in the pure InAs dot (larger band offsets). This trend has also been observed experimentally (Fig. 7 in Ref. 6).

The splitting η of the dark states. These splittings are small for all the considered dots. They are introduced through two different effects. First, when the hole states pick up some Γ_{1v} character from the valence $|Z\rangle$ band (neglected in the simple model). Such mixing exists even for dots of C_{2v} symmetry and is expected to be stronger in *tall* dots, where the confinements in the z and in the x-y directions are comparable. In this case, η is proportional to the z-polarized dipole oscillator strength of the upper dark state. Second, for dots of lower symmetry (alloyed or shape asymmetric), mixing of dark and bright states becomes allowed and we expect larger splittings with dark states of x-y polarization as well as z polarization. Taking these effects into account, the new exchange Hamiltonian is given by H'_{ex} [Eq. (1)] and has the eigenvalues depicted in Fig. 3(d). For the dots presented, η is very small.

In summary, we explain the origin of FS splittings by developing a model based on symmetry considerations. We use this model to analyze the numerical results obtained for $\mathrm{In}_{1-x}\mathrm{Ga}_x\mathrm{As}$ dots of various shapes and compositions (tall, flat, elongated, pure, and alloyed). We observe and explain the occurrence of polarization anisotropy and FS splittings in lens-shaped dots (even with a perfectly circular base) and reveal trends in the calculated FS.

This work was supported by the U.S. Department of Energy and SC-BES-DMS Grant No. DEAC36-98-GO10337.

[1] D. Gammon *et al.*, Phys. Rev. Lett. **76**, 3005 (1996).
[2] D. Gammon *et al.*, Science **273**, 87 (1996).
[3] L. Landin *et al.*, Science **280**, 262 (1998).
[4] M. Bayer *et al.*, Phys. Rev. Lett. **82**, 1748 (1999).
[5] M. Bayer *et al.*, Phys. Status Solidi A **178**, 297 (2000).
[6] M. Bayer *et al.*, Phys. Rev. B **65**, 195315 (2002).
[7] M. Sugisaki *et al.*, Phys. Rev. B **59**, R5300 (1999).
[8] S. Cortez *et al.*, Phys. Rev. B **63**, 233306 (2001).
[9] M. Paillard *et al.*, Phys. Rev. Lett. **86**, 1634 (2001).
[10] A. Franceschetti *et al.*, Phys. Rev. B **60**, 1819 (1999).
[11] C. Pryor *et al.*, J. Appl. Phys. **83**, 2548 (1998).
[12] G. Bastard, *Wave Mechanics Applied to Semiconductor Heterostructures* (Halstead, New York, 1988).
[13] A. Zunger, Phys. Status Solidi B **224**, 727 (2001).
[14] L.-W. Wang *et al.*, Phys. Rev. B **59**, 5678 (1999).
[15] L.-W. Wang and A. Zunger, Phys. Rev. B **59**, 15 806 (1999).
[16] A.J. Williamson *et al.*, Phys. Rev. B **62**, 12 963 (2000).
[17] G.F. Koster *et al.*, *Properties of the Thirty-Two Point Groups* (MIT Press, Cambridge, MA, 1963).